Anal. Chem. **2007,** *79,* 9160−9165

Micromachined Bradbury−Nielsen Gates

Ignacio A. Zuleta, Griffin K. Barbula, Matthew D. Robbins, Oh Kyu Yoon, and Richard N. Zare*

Department of Chemistry, Stanford University, Stanford, California 94305-5080

Bradbury−Nielsen gates (BNGs) are a standard way for gating or steering beams of charged particles in ion mobility spectrometry and time-of-flight mass spectrometry. They consist of a pair of interleaved electrodes that when at the same potential allow ions to pass through the electrodes undeflected and, when a voltage is applied, cause the ions to be deflected from their propagation axis. Previous efforts to construct such devices have relied on mechanical assembly by winding wires across an aperture. We describe a micromachining method for making monolithic BNGs using deep reactive ion etching of silicon-on-insulator wafers. This method enables the creation of electrodes with spacings ranging from 25 to 100 μm with a thickness of 20 μm, covering a 5 mm by 5 mm active area. We characterize the performance of these micromachined BNGs by ion imaging in a pseudo-random time-of-flight mass spectrometer.

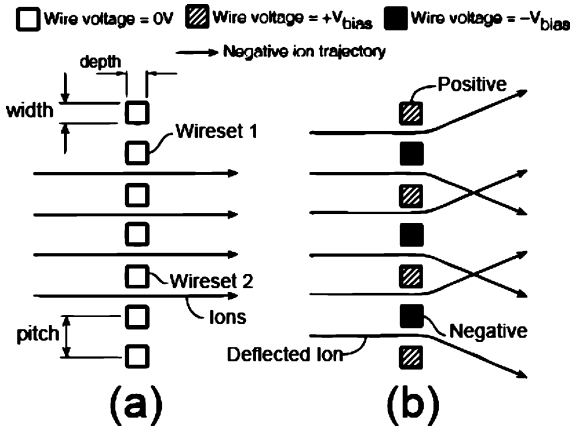

Figure 1. Mode of operation of a Bradbury−Nielsen gate. (a) When no voltage is applied across the electrodes or wires, ions can cross the gate undeflected. (b) When a voltage V_{bias} is applied. ions are deflected off-axis giving rise to two beamlets.

In chemical analysis using ion mobility spectrometry (IMS) or time-of-flight mass spectrometry (TOF-MS), the distribution of arrival times at a detector is measured for ions associated with molecules present in a sample. This arrival time distribution is a proxy for the distribution of collision cross sections or mass-to-charge ratios of the ions. In both IMS and TOF-MS, an ion beam is gated using time-dependent transverse electrical fields according to waveforms of varying duty cycle. In linear gating schemes, such as in IMS[1−4] or Hadamard transform mass spectrometry[5] (HT-TOF-MS), the gating is accomplished by a pair of interleaved deflection plates that deflect the ion beam off-axis. This pair of interleaved deflection plates used for axial gating of an ion beam is referred to as a Bradbury−Nielsen gate (BNG).[6] Depending on the kinetic energy of the incoming ions, the strength of the electric field applied, and the presence or absence of collisions, the ion beam may fail to strike the detector because it is either completely neutralized at the electrodes or deflected off axis.

The gate consists of two interleaved sets of electrodes that lie in a plane normal to the ion beam trajectory (Figure 1). To deflect ions, a voltage difference is applied between the electrode sets. Because of the periodic nature of the dipole motif, the deflection field quickly decays with distance from the BNG plane (about one wire spacing) and the device looks like a grid at the average voltage between the two wires. When voltage is applied, the deflection field is significant only inside the gap between the electrodes and the narrow adjacent volume.

There are a number of advantages to this geometry compared to traditional deflection plates: short transit times, high sensitivity, and high beam admittance. The characteristic short transit time derives from the short length of the BNG deflection region (~100 μm for a 100-μm gate) compared to traditional deflection plates (few cm). Also, because of the small distance between electrodes, fields inside a BNG active area can easily be in the order of 10^5 V/m when just tens of volts are applied to it, making the deflection angle very sensitive to the voltage applied. Finally, because of its extended geometry, large portions of a macroscopic ion beam entering a BNG are transmitted and deflected individually as they travel through different electrode gaps. These unique properties allow for fast gating or modulation of a macroscopic ion beam. Besides IMS and HT-TOF-MS, BNGs have been used as ion gates in other MS-related high-speed applications such as mass selection gates in orthogonal extraction TOF mass spectrometers and in tandem TOF/TOF mass spectrometers.[7,8]

In its most common implementation, BNG electrodes are metal wires supported by a solid insulator having a central opening that defines the device's active area.[9,10] These gates have the advantage

* To whom correspondence should be addressed. E-mail: zare@stanford.edu.

(1) Nielsen R. A., Bradbury N. E. *Phys. Rev.* **1937**, 51, 69−75.
(2) Borsdorf, H., Eiceman G.A. *Appl. Spectrosc. Rev.* **2006**, 41 (4), 323−375.
(3) Spangler, G. E. *Anal. Chem.* **1993**, *65*, 3010−3014.
(4) Steiner, W. E.; Clowers, B. H.; Fuhrer, K.; Gonin, M.; Matz, L. M.; Siems, W. F.; Schultz, A. J.; Hill, H. H. *Rapid Commun. Mass Spectrom.* **2001**, *15* (23), 2221−2226.
(5) Brock, A.; Rodriguez, N.; Zare, R. N. *Anal. Chem.* **1998**, *70* (18), 3735−3741.
(6) Bradbury, N. E.; Nielsen, R. A. *Phys. Rev.* **1936**, *49*, 388 − 393.
(7) Beussman, D. J.; Vlasak, P. R.; McLane, R. D.; Seetedin, M. A.; Enke, C. G. *Anal. Chem.* **1995**, *67*, 3952−3957.
(8) Cotter, R. J.; Gardner, B. D.; Iltchenko, S.; English, R. D. *Anal. Chem.* **2004**, *76*, 1976−1981.

10.1021/ac071581e CCC: $37.00
Published on Web 10/30/2007

of relatively fast construction (hours) and virtually unlimited active area size. In this approach, wires are preloaded with a given amount of tension to stay straight and they are aligned with the aid of a machined template. Because the precision in the electrode positions relies strongly on the machining precision of external templates needed to guide the wires during construction and because metals are softer than single crystals, it proves challenging to use wire that is smaller than 10 μm in diameter with spacing smaller than 100 μm to create stiff structures that can withstand high temperatures.

In contrast, bulk silicon can be doped to become conductive and metallized if needed. Moreover, it is exceptionally rigid, which makes silicon ideal for creating high aspect ratio, free-standing structures in a short time (1−2 days). In particular, with the advent of SF_6/C_4F_8 deep reactive ion etching (DRIE) of silicon using the Bosch process,[11] aspect ratios of 30:1 can readily be achieved. DRIE has successfully been used to make miniature Einzel lenses,[12] electron beam blankers,[13] electron beam lithography columns,[14] analog-to-digital converters,[15] and electron microscopes. Moreover, ion trap,[16,17] quadrupole,[18,19] and ion mobility spectrometers[20,21] have been microfabricated using reactive ion etching of silicon. We demonstrate that this technology has the potential to help make robust BNGs as well as to enable high-performance BNGs with smaller electrode spacings. Here we describe a method for fabrication of silicon ion gates for time-of-flight mass spectrometry using DRIE of silicon-on-insulator (SOI) wafers. We then demonstrate their ion beam modulation performance.

EXPERIMENTAL SECTION

Microfabrication. Figure 2 shows the overall process used to fabricate the devices. All mask designs and mask writing were done in-house. The masks were drawn using Tanner's L-Edit software. The SOI wafer (MEMS Engineering Inc., Fremont, CA) had a 20-μm Si(100) antimony-doped layer (R < 0.01 Ω cm) bonded to a 400-μm Si(100) boron-doped handle (R < 1 Ω cm). The buried oxide layer was 0.5 μm thick.

The first step to delineate the electrodes onto the front side of the SOI wafer is deposition of an aluminum layer (Figure 3a).

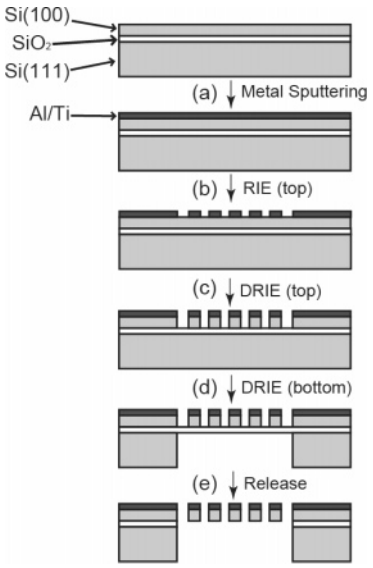

Figure 2. BNGs obtained after a series of microfabrication steps including (a) metallization, (b) metal etching, (c) DRIE of the top side to define the wires, (d) DRIE of the bottom layer to open up a window, and (e) release of the free-standing wires by wet etching of the supporting buried oxide layer.

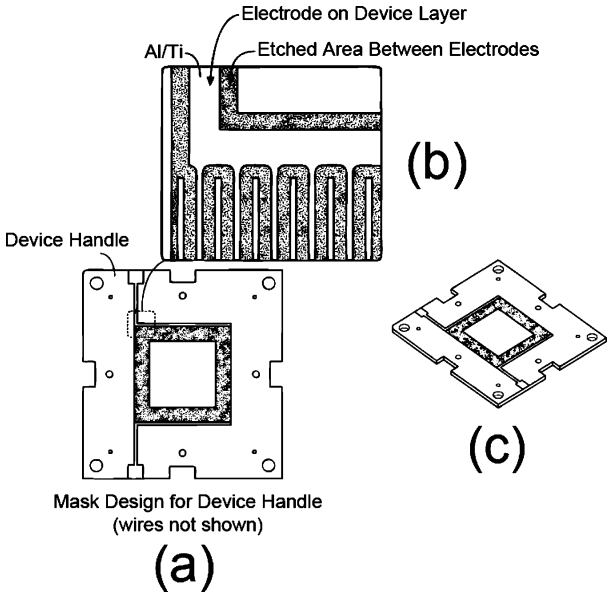

Figure 3. Mask for the device designed and including (a) a window defining the active area as well as (b) the electrode positions. (c) A 3D mechanical model was done to ease assembly into the mass spectrometer.

Prior to deposition, the wafers are thoroughly cleaned to remove organics, metals, and the native oxide layer present on the Si surface. SOI surfaces are further cleaned using ion milling to remove ~7 nm of material. Titanium and aluminum are deposited using a Gryphon metal sputtering system on the clean wafers to form the conductive surface of the future electrodes. The titanium is deposited first to improve adhesion and to ensure low resistance between the aluminum film and the silicon substrate. Aluminum is deposited to prevent charging of the electrodes and to facilitate welding. A 0.5-μm layer of Ti is deposited at an argon gas base pressure of 1.7×10^{-7} Torr at 2 kW power for 240 s. A 2-μm layer of Al is then deposited at a pressure of 2.4×10^{-3} Torr at 7.5 kW power for 1200 s.

(9) Kimmel, J. R.; Engelke, F.; Zare, R. N. *Rev. Sci. Instrum.* **2001**, *72* (12), 4354−4357.
(10) Yoon, O. K.; Zuleta, I. A.; Robbins, M. D.; Barbula, G. K.; Zare, R. N. *J. Am. Soc. Mass Spectrom.* **2007**, *19*, 1901–1908.
(11) Laermer, F.; Schlip, A. U.S. Patent 5501893.
(12) Syms, R. R. A.; Michelutti, L.; Ahmad, M. M. *Sens. Actuators, A* **2003**, *107*, 285−295.
(13) Winograd, G.; Krishnamurthi, V.; Garcia, R.; Veneklasen, L. H.; Mankos, M.; Pease, F. *J. Vac. Sci. Technol., B* **2000**, *18* (6), 3052−3056.
(14) Chang, T. H. P.; Thomson, M. G. R.; Kratschmer, E.; Kim, H. S.; Yu, M. L.; Lee, K. Y.; Rishton, S. A.; Hussey, B. W.; Zolgharnain, S. *J. Vac. Sci. Technol., B* **1996**, 14 (6).
(15) Ioakeimidi, K.; Leheny, R. F.; Gradinaru, S.; Bolton, P. R.; Aldana, R.; Ma, K.; Clendenin, J. E.; Harris, J. S.; Pease, R. F. W. *IEEE Trans. Microwave Theory Tech.* **2005**, *53* (1), 336−342.
(16) Stick, D.; Hensinger, W. K.; Olmschenk, S.; Madsen, M. J.; Schwab, K.; Monroe, C. *Nat. Phys.* **2006**, *2* (1), 36−39.
(17) Blain, M. G.; Riter, L. S.; Cruz, D.; Austin, D. E.; Wu, G.; Plass, W. R.; Cooks, R. G. *Int. J. Mass Spectrom.* **2004**, *236*, 91−104.
(18) Geear, M.; Syms, R. R. A.; Wright, S.; Holmes, A. S. *J. Microelectromech. Syst.* **2005**, *14* (5), 1156−1166.
(19) Taylor, S.; Tindall, R. F.; Syms, R. R. *J. Vac. Sci. Technol., B* **2001**, *19* (2), 557−562.
(20) Miller, R. A.; Nazarov, E. G.; Eiceman, G. A.; King, T. A. *Sens. Actuators, A* **2001**, *91*, 301−312.
(21) Krebs, M. D.; Zapata, A. M.; Nazarov, E. G.; Miller, R. A.; Costa, I. S.; Sonenshein, A. L.; Davis, C. E. *IEEE Sens. J.* **2005**, *5* (4), 696−703.

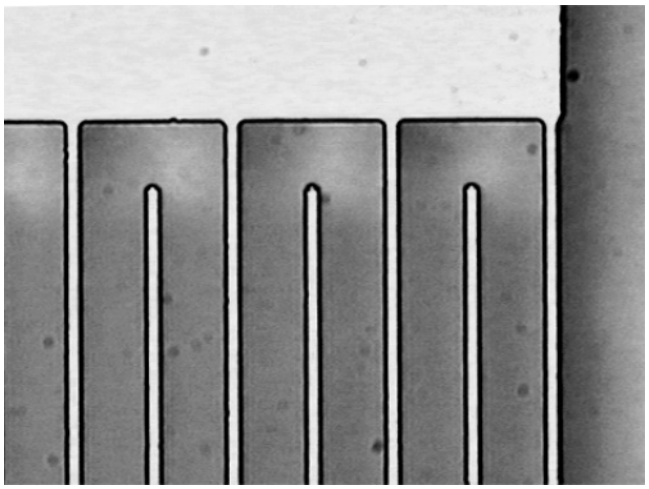

Figure 4. Detailed photograph of a BNG that has been subjected only to top side deep reactive ion etching. Clear areas represent the raised metallized electrodes and darker areas represent the exposed buried oxide layer.

The metallized wafers are masked to pattern the electrodes onto the aluminum layer. For this purpose, a 1.6-μm-thick layer of Shipley 3612 resist is spun onto the wafers. Using a Karl Süss MA-6 contact aligner, the wafers are exposed for 1 s using the top mask (λ = 365 nm, 15 mW/cm^2). Afterward, they are developed (Shipley LDD-26W) for 180 s and hard-baked for 90 s at 115 °C to strengthen the resist. Aluminum is patterned using resist as the mask using a Cl_2 plasma (P5000, Applied Materials, Santa Clara, CA), and the wafers are rinsed with DI water immediately afterward (Figure 3b). At this point, features are already patterned on the top layer by the remaining Al/Ti layer. Using this metal layer as a mask (Figure 3c), the wires are defined by a 32-min DRIE on a SF_6 inductively coupled plasma (ICP) etcher (ICP Multiplex, Surface Technology Systems, Newport, UK). Figure 4 shows the resulting structures; wires appear light against a darker purple background of SiO_2. To remove traces of resist, the wafer is subjected to a 4-min cleaning in an oxygen−plasma asher and a subsequent wet resist strip (PRX-127, SVC Corp.) bath.

After the front side has been machined, it is protected from scratches with a 7-μm-thick layer of resist (SPR220-7, Shipley) spun for 5 s at 500 rpm. The resist is baked for 30 min at 110 °C to enhance bonding. The mask is aligned with the features on the topside of the wafer and exposed for 13 s (λ = 365 nm, 15 mW/cm^2). After exposure, the wafers are baked for 45 min at 110 °C to harden the resist so that it withstands the long, deep etch. The wafers were developed (Shipley LDD-26W) for 5 min. A carrier wafer is first manually coated with a 1.6-μm layer of Shipley 3612 resist and placed face up beneath the device wafers so that the flats are aligned. They are then pressed against each other for 1 h at 105 °C on a hot plate.

Using the same DRIE process that defined the wires, the back window is etched for 4 h in 30-min increments using the buried oxide layer as an end point (Figure 3d). The released wafer is then carefully cleaned and stripped of resist. Etching away the buried oxide layer requires the use of an HF-based etchant that has selectivity against aluminum (Figure 3e). "Pad-etch" is an HF-based etchant containing acetic acid that only etches aluminum ~40 nm in the first few minutes (up to 70 nm after 30 min) and then slows down because of passivation. In contrast, SiO_2 is etched at a constant rate of 22 nm/min or faster.

Once the devices, still in the wafer, have been released using the oxide wet etch, they are air-dried, and they easily break apart into individual dies. For normal operation, the devices are bonded to a custom-made, gold-plated printed circuit board (PCB). The whole process to complete a batch of devices takes 17 h of clean room time, over which two 4-in. wafers, containing 12 devices each, can be processed.

Mass Spectrometry. Electrospray ionization was used to deliver a 2 mM tetrabutylammonium (Sigma Chemical, St. Louis, MO) solution into the instrument. The sample is dissolved in a 50:50 v/v mixture of high-purity water and methyl alcohol (Aldrich Chemical, Milwaukee, WI) with 0.001 M acetic acid (Aldrich) added. The ion source consists of a heated capillary operated at 270 °C followed by an off-axis skimmer and a quadrupole ion guide operated at 2.94 Mhz and 150 V(peak-to-peak). After accelerating ions to 1.5 keV, the ion deflection experiments are performed in an 82-cm-long flight tube, which is at a pressure of 2.0×10^{-7} Torr. Ions were imaged using a microchannel plate detector fitted with a P22 phosphor screen (Burle Electro-Optics Inc., Sturbridge, MA). Images were recorded using a standard CCD camera and frame grabber (NI PCI-1409, National Instruments, Austin, TX). Ions reaching the center of the detector were counted using a time-to-digital converter (model P7888/6, FastComTEC, Oberhaching, Germany) and a 2-mm skimmer in front of the detector.

Table 1. Some Mechanical Properties of Silicon and Tungsten[a]

	Si	W
yield strength (GPa)	700	600
Knoop hardness (kg/mm^2)	850	485
Young's modulus (GPa)	129.5 [100] 168.0 [110] 186.5 [111]	410
density (g/cm^3)	2.3	19.3
thermal conductivity (W cm^{-1} K^{-1})	1.57	1.78
thermal expansion coefficient (10^{-6} K^{-1})	2.33	4.50

[a] Reference 23.

RESULTS AND DISCUSSION

Our first step in designing and micromachining a BNG is the choice of a mechanical substrate to define the electrodes. This material should be strong enough to sit across an aperture without sagging or deforming under the forces developed during either fabrication or operation. The material can be either crystalline, like single-crystal silicon (SCS), or metallic, like tungsten, which is the usual material used to make wire-based BNGs. The selection of high-purity SCS as the semiconductor of choice for microelectronics was based on both its electronic and mechanical properties. Table 1 compares some mechanical properties of silicon and of tungsten. Table 1 shows that SCS is harder (high Knoop hardness), more flexible, lighter (lower density), a comparable heat conductor, and less sensitive to temperature change (smaller thermal expansion coefficient).[22−24] Also, because of its crystalline structure and lack of grain structure, it does not exhibit inelastic

(22) Petersen, K. E. *Proc. IEEE* **1982**, *70*, 5, 420−469.
(23) Madou, M. J. *Fundamentals of Microfabrication*; CRC Press: Boca Raton, FL, 2002.
(24) Greenwood, J. C. *J. Phys. E: Sci. Instrum.* **1988**, *21*, 1114−1128.

Table 2. Some Properties of the Microfabricated BNGS

	20/80	10/40	5/20
active area (mm^2)	25	25	25
thickness (μm)	400	400	400
electrode depth (μm)	20	20	20
electrode width (μm)	20	10	5
electrode gap (μm)	80	40	20
electrode pitch (μm)	100	50	25
capacitance (pF)	128	178	207
transmission (%)	80	80	80

deformation or fatigue under load, which means that electrodes constructed with it will not loosen over time or at high temperature like metals do. These mechanical properties together with the availability of lithography and DRIE make silicon an ideal substrate to create the electrodes that make up a BNG.

Several micromachining techniques are available for the etching of silicon. One can either wet etch silicon along its crystal planes, deposit, and pattern a thin film or use dry etching on bulk silicon. Because it combines the advantages of both thin film processing and dry etching, we decided to machine the new beam modulation device employing SOI bulk micromachining. SOI wafers consist of a three layers: a thin Si "device" layer (10−50 μm), usually a few micrometers thick, an insulating "buried oxide" SiO_2 layer (0.01−2 μm), and a thick Si handle (400 μm). The fact that conductive Si is used for the handle as well as for the device layer prevents charge buildup and allows the devices and the handle to be electrically connected. The fabrication process has two main stages: delineation of the wires on the device layer and etching of a window from the back, also known as the "release" step. These tasks are accomplished with a combination of masking and DRIE for both the device and the window, as described in the Experimental Section. Our BNG structure, shown in Figure 3, consists of two free-standing sets of electrodes and resembles an interdigitated capacitor. These electrodes are mounted on a Si handle from which they are electrically isolated by a thin SiO_2 layer. The Si body provides a ground plane and hides from the ions the electrical field generated by the connection pads.

Several different kinds of BNGs were designed with a variety of distances between electrodes and electrode widths. Table 2 shows some properties of the different gates successfully made with the technique described here. The electrode width/electrode gap combinations explored were 5 μm/20 μm, 10 μm/40 μm and 20 μm/80 μm, with a transmission of 80% in each case. In all cases, the active area, that is, the area of the device exposed to the ion beam, was a 5 mm by 5 mm square window. The devices are 15 mm × 15 mm × 400 μm silicon dies with windows exposing electrodes from the back. The electrodes are Al-coated silicon structures insulated from the silicon bulk body by an insulating 500-nm SiO_2 glass layer. The device has provisions for different mounting schemes, including holes for either glass fiber or sapphire ball type of alignment, for a position accuracy of 1 μm or better. This feature allows for stacking several optical elements that share the same mounting scheme in an integrated ion modulation column that could include microfabricated lenses and grids.

Figure 5b shows the resulting electrodes after release. It can be seen that for some devices (~30%) wires can be missing or stuck together. Inspection with SEM reveals the nature of these defects and allows us to discard imperfect devices. Common

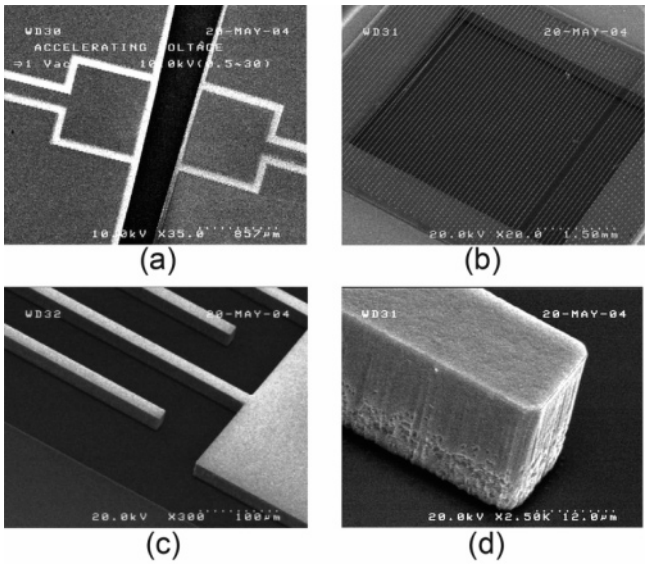

Figure 5. SEM images of microfabricated gates. The gates are interfaced to the outside by (a) connection pads. SEM inspection helps detect (b) nonworking gates with missing or bundled wires. Aspect ratio and shape of the electrodes is effectively determined by the DRIE process, giving rise to (c) electrodes well isolated from each other and to (d) steep sidewalls.

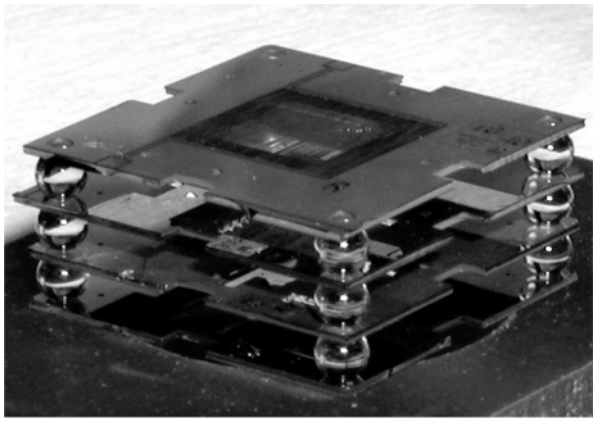

Figure 6. Finished 100-μm microfabricated gate shown stacked with other silicon electrodes using sapphire spheres (±0.000 005 in. tolerance).

defects arise from remains of hardened resist found across electrodes, rupture of electrodes during the final drying, wire ends coming loose from overetching during release and the "footing" effect during DRIE. Figure 5d shows in detail the end of one of the electrodes, including the sidewall grooves characteristic of the Bosch process as well as the footing effect. This effect that can be seen at the bottom of the electrode results from the sideways etching of the electrode caused by the charging up of the exposed SiO_2 layer when the etch process nears the end point.[25−28] The BNG gates are connected to the driving electronics by bonding them to a printed circuit board and pressing indium wire between the pads (Figure 5a) and the PCB. Figure 6 shows a device after all processing has been completed.

(25) Arnold, J. C.; Sawin, H. H. *J. Appl. Phys.* **1991**, *70*, 5314−5317.
(26) Hwang, G. S.; Giapis, K. P. *J. Vac. Sci. Technol., B* **1997**, *15*, 70−87.
(27) Murakawa, S.; Fang, S.; McVittie, J. P. *Appl. Phys. Lett.* **1994**, 64, 1558−1560.
(28) Giapis, K. P. *J. Vac. Sci. Technol., B* **1997**, 15, 70−87.

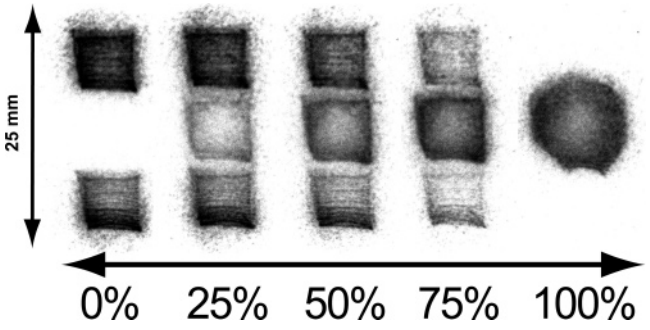

Figure 7. Ion image of a TBA^+ (*m*/*z* 242) ion beam modulated at different duty cycles. Darker areas indicated higher ion current density. Deflection voltage is ±17 V, and ion energy is 1500 eV.

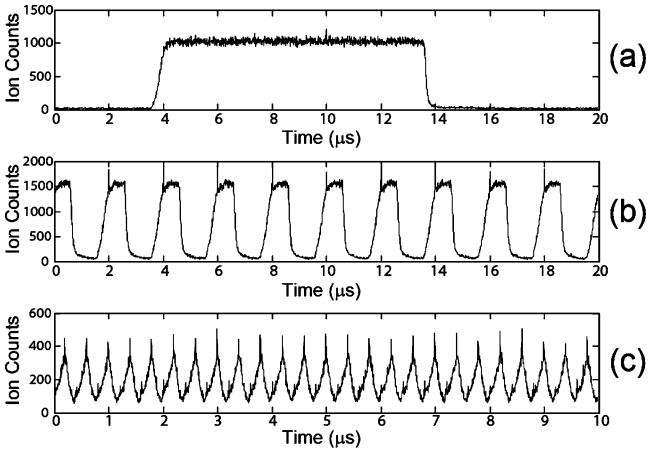

Figure 8. Ion packets created using a microfabricated gate modulated at (a) 100 kHz, (b) 1 MHz, and (c) 5 MHz. At higher frequencies behavior is limited by the response time of the driving electronics.

Gating Performance. The gate used in these studies has electrodes 20 μm deep and 20 μm wide that are 100 μm apart from each other. We tested the performance using a beam of tetrabutylammonion ions, (TBA^+, *m*/*z* 242) created using electrospray ionization at various frequencies with a train of equally spaced pulses. Time-averaged ion beam images first acquired at the detector plane show that the beam is split when a 100-kHz pseudorandom sequence of ±17 V pulses is applied to the wires at various duty cycles. At 0% duty cycle, the gate is off all the time, and at 100%, the ion beam is on all the time, provided that we are recording ions at the center area (Figure 7). Note that the blurring observed for the undeflected ion beam, which arises from a slight charge up of the wires when no sequence is applied, is caused by the driving electronics ability to source charge when idle and should not affect performance of the devices.

The ability of the BNG to time-stamp an ion beam mainly depends on two factors: its ability to deflect the ion beam completely out of a detection region[29] and its response time. What is usually desired is that the modulated ion current measured at a particular point in the detector plane is a two-valued function of time with detectable "on" and "off" states. That is, for a given point in the detector and when only one ion type is present, ion current is ideally either high or low. The ion current at the detector is determined by the instantaneous overlap of the ion beam and the detection region at the detector plane for a given deflection angle. The field experienced by the ions is proportional to a time-varying voltage $V(t)$ applied to the BNG during operation.[30] The deflection angle is ideally proportional to this voltage and decreases with higher acceleration voltages and wider electrode spacings. For example, the ion beam shown in Figure 7 is deflected ~0.0006 rad/V applied to the BNG.

The response time of the BNG depends on the characteristic size of the ion beam and detector, the rise time of the electronics,

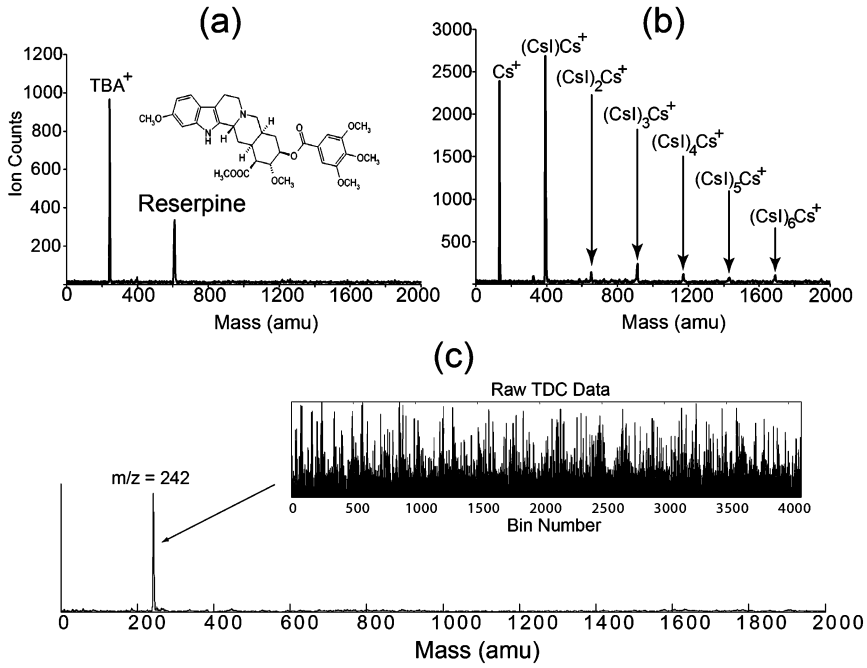

Figure 9. Mass spectra acquired with the microfabricated BNGs in conventional mode, with a single ion packet, for common substances like (a) reserpine and (b) cesium iodide complexes. (c) Hadamard transform time-of-flight spectra were acquired by modulating the ion beam at 10 MHz with a 12-bit PRBS. The inset shows the raw data before demodulation.

the voltage applied, the electrode gap, and the electrode depth. The electronics used in these experiments are placed outside the vacuum chamber far from the BNG, use wires to apply the voltages, and thus exhibit a rise time of ~100 ns. Nevertheless, we find that the BNG is capable of faithfully deflecting an ion beam under these operating conditions. By examining the ion current close to the center area, using a skimmer to mask off-axis ions, we find that the ion beam has been temporally encoded when the packet width is large compared to the rise time. This means that, if we applied a two-valued voltage signal to the BNG, the ion current signal that is measured is essentially two-valued as well. Figure 8 shows ion packets successfully created by applying a sequence of on and off pulses of equal amounts (50% duty cycle) at various frequencies. As can be seen in this figure, the modulation behavior at high frequency is dominated by the finite rise time in our current setup and should be interpreted as a lower limit on the speed of the devices

Mass Spectrometry. To test the microfabricated BNGs, we acquired spectra in both conventional and HT-TOF-MS mode. To measure mass spectra in what we term "conventional mode", we create an ion packet by only turning on the ion beam for a short period of time. Figure 9a shows a spectrum of reserpine and TBA acquired by creating a single 100-ns pulse. Also, we show in Figure 9b a spectrum of cesium iodide complexes acquired under the same conditions. Although performance of these gates is limited by the driver electronics, we have successfully created 14-ns packets that correspond to a resolution of 750 (fwhm) when using higher acceleration voltages (2000 V) and high frequencies (40 MHz).

In a HT-TOF-MS experiment, ions entering a time-of-flight mass spectrometer are directed onto a BNG. Figure 1 describes the principle under which the gate operates in this technique: the BNG deflection voltage is rapidly modulated on and off with a known sequence, creating small packets of ions deflected to different extents off the propagation axis. All ions enter the flight tube, but discrete packets are defined for a given angle off the axis. The ion current measured at a particular angle can be thought of as being the superposition of the TOF spectra for each packet. An underlying TOF distribution that would elicit the measured time trace is then computed and used to obtain the mass spectrum of the sample. The recovered signal is equivalent to conventional TOF spectrum, but has an improved signal-to-noise ratio owing to the modulation−demodulation multiplexing scheme.[31]

Ion current time traces were acquired for a 10 MHz, 12-bit pseudorandom binary sequence (PRBS)-modulated TBA^+ ion beam impinging on a microchannel plate detector. As modeled, the gates successfully encoded the ion beam and enabled the acquisition of HT-TOF spectra as can be seen in Figure 9c. Because the driving electronics for these spectra are outside the instrument, rise time and ringing create packets of varying heights, when compared to the rather binary modulation expected when there is no electronic noise and there is only one substance.

Our experiments with the described MEMS-based BNGs show a unique potential for implementing fast and accurate ion gates. We have described a process flow and successfully demonstrated the performance of these devices as well as a general method for fabrication of ion optical devices based on SOI micromachining. The microfabricated devices are mechanically robust and have spacings that are equal or smaller than previously reported using prior technology. Also, preliminary characterization of the simplest configuration indicates that performance will most probably be found to increase for the more closely spaced configurations. This work represents a novel application of recent micromachining technologies to the fabrication of mass spectrometry ion optics. Although we can only speculate about the exciting long-term implications of these developments, we suggest that that they will prove useful in the pursuit of mainstream high-duty-cycle mass spectrometry and ion mobility spectrometry.

ACKNOWLEDGMENT

Special acknowledgment is given to all Stanford Nanofabrication Facility/Center for Integrated Systems lab members. I.A.Z. especially thanks Eric Peroziello (SNF) and Dan Pickard (CIS, Pease Group), who gave valuable advice and support when developing the specifications and the fabrication process. Also, special acknowledgment is given to the material and technical help provided by Ray Cochran of Burle Electrooptics, Inc., who provided the ion beam imaging hardware used in this project. This material is based on research sponsored by the Air Force Research Laboratory, under STTR contract C05-0710-01.[32] Work was performed in part at the Stanford Nanofabrication Facility (a member of the National Nanotechnology Infrastructure Network), which is supported by the National Science Foundation under Grant ECS-9731293, its lab members, and the industrial members of the Stanford Center for Integrated Systems.

Received for review July 26, 2007. Accepted September 5, 2007.

AC071581E

(29) Yefchak, G. E.; Schultz, G. A.; Allison, J.; Enke, C. G.; Hollande, J. F. *J. Am. Soc. Mass. Spectrom.* **1990**, *1*, 440−447.

(30) In a real experimental setup, the voltage at the BNG wires differs from the unamplified signal applied due to the finite output impedance of the driving electronics, the cable inductance, and the sum of all capacitances present. In this case, we would need to establish the equivalent RLC circuit and apply the corresponding frequency filter to the voltage time trace using the Laplace transform.

(31) Kimmel, J. R.; Yoon, O. K.; Zuleta, I. A.; Trapp, O.; Zare, R. N. *J. Am. Soc. Mass. Spectrom.* **2005**, *16*, 1117−1130.

(32) The U.S. Government is authorized to reproduce and distribute reprints for Governmental purposes notwithstanding any copyright notation thereon. The views and conclusions contained herein are those of the authors and should not be interpreted as necessarily representing the official policies or endorsements, either expressed or implied, of the Air Force Research Laboratory or the U.S. Government.